JOURNAL OF MATERIALS SCIENCE 26 (1991) 3275–3286

Cyclic fatigue of ceramics

F. GUIU, M. J. REECE*, D. A. J. VAUGHAN
Department of Materials, Queen Mary and Westfield College, Mile End Road, London E1 4NS, UK

The fatigue behaviour of alumina, zirconia-toughened alumina (ZTA) and tetragonal zirconia (TZP) have been investigated using three different techniques. Direct push–pull testing has been used to generate both static and cyclic fatigue data. The results clearly show that all the materials studied are susceptible to both static and cyclic fatigue, and that the times to failure under cyclic loading are considerably shorter than under static loads. The fatigue failure origins have been identified and the influence of surface condition on fatigue life has been assessed. The slow propagation of cracks subject to cyclic tensile and compressive loads has been studied using compact tension specimens and tapered double cantilever beam specimens. These investigations have confirmed the existence of cyclic fatigue effects in coarse-grained alumina and have shown the crack increment per cycle (da/dN) to have a power-law dependence on the peak stress intensity factor. A technique, based on repeated indentation, has been used to investigate the propagation of sub-surface cracks subjected to cyclic loading in both fine-grained alumina and ZTA. The results of the investigation suggest that compressive or closure loads on the crack faces are factors which affect the cyclic fatigue crack growth in ceramics. Based on those observations, an explanation is proposed for the mechanical cyclic fatigue effects in the ceramics investigated.

1. Introduction

The problem of fatigue failure by the slow propagation of cracks under cyclic loads is of paramount importance, and has been widely studied in metals and ductile materials where subcritical cracks grow by processes of localized plasticity at their tips. Because ceramic materials exhibit very limited plasticity at room temperature, this aspect of their mechanical properties has remained largely unexplored until recently. Evidence for the existence of real mechanical fatigue effects in brittle ceramics has existed for some time [1–7], but despite this there has been a widespread belief that the slow propagation of cracks under cyclic stresses could be explained by the same environmental and corrosive processes responsible for subcritical crack growth under steady loads [8–10]. This view may have been reinforced by the fact that some of the earlier work on cyclic fatigue of brittle materials was conducted on glass which may not be as susceptible to cyclic fatigue as some of the more recently studied polycrystalline ceramics. Because of this conception, the term "fatigue" when applied to ceramics has often been used in the past to mean the slow growth of cracks under constant loads, whilst the term "dynamic fatigue" has been applied to describe the stress-rate-dependent failure under monotonic loading. More recently, the terminology has become more specific and consistent with that in common use in materials science: the term static fatigue is applied to failure under constant load, whilst cyclic fatigue is used to describe the slow growth of cracks and ultimate failure under cyclic loads.

Another possible reason for the paucity of investigations of the effect of cyclic stresses on the fatigue behaviour of ceramics in the past may be the inherent difficulty involved in subjecting brittle materials to this mode of testing. The simplest method of investigating the effect of reversed stresses on the fatigue behaviour of a material is probably direct push–pull, but this is also the most difficult and demanding in terms of alignment, specimen perfection and machining cost when it is applied to a brittle material. In the scientific literature there are very few fatigue studies of ceramics in direct push–pull, although they have provided some of the evidence for the existence of mechanical fatigue effects in alumina ceramics [6, 11].

Most of the early studies of cyclic fatigue in ceramics, glasses and rocks were conducted using techniques which subjected the specimens to cyclic tensile stresses such as repeated bending of a beam [3, 4, 7, 12], and double torsion [8, 9]. A notable exception is the work of Williams [1, 2] conducted in rotating bending, this being possibly the earliest work on record on cyclic fatigue of ceramics where fully reversed cyclic stressing was used.

There has been recently a growing interest in the behaviour of ceramics under cyclic fatigue conditions, and results obtained by different workers using different techniques and materials have shown conclusively the existence of mechanical fatigue effects which are

* *Present address*: National Physical Laboratory, Teddington, Middlesex, UK.

0022–2461/91 $03.00 + .12

independent of environmental factors. Several different techniques and ceramic materials were used in these recent studies. Measurements of the fatigue life of silicon nitride [13, 14], magnesia, partially stabilized zirconia (Mg–PSZ) [15] and alumina [16] have been carried out under cyclic flexure [13] and in rotation bending [14–16]. Crack-growth rates have been measured in Mg–PSZ [17–19] and in Al_2O_3–SiC composite by repeated tensile loading [20] and in a coarse grain alumina by tension–compression loading [21] using compact tension specimens. Direct push–pull has been used to determine the fatigue lives of some aluminas [6, 11] and SiC reinforced with SiC fibres [22]. The growth of fatigue cracks from the root of notches under repeated far-field compression has been shown to be an important fatigue-crack-growth mechanism for a variety of monolithic and composite ceramic materials [23–26]. Recently the growth of fatigue cracks in tension has been studied from holes in compressively loaded bars [27].

Some possible mechanisms of subcritical crack growth by fatigue in brittle ceramics were first suggested and discussed by Evans [10] in his review of the few results available at the time. Cyclic fatigue effects and the conditions that promote them are now much better documented and it is generally accepted that they are all dependent on the polycrystalline nature of the ceramic materials and are based on the existence of some strain irreversibility on stress reversal. In repeated far-field compression loading the strain irreversibility at the root of notches is believed to arise from the incomplete reverse sliding of the faces of microcracks produced at the notch tips [24, 26], or from the irreversible transformation strains which occur in transformation-toughened ceramics [26]. These irreversibilities give rise to residual tensile stresses at the notch tip (similar to those produced by plasticity in metals) which can help to open cracks in a combination of modes I and II.

There may exist other sources of strain irreversibility which would be more relevant to fatigue-crack growth under cyclic tensile loads. For example, the relaxation of internal stresses on microcracking and the wedging and frictional sliding of asperities on the crack faces have been proposed as alternative sources of strain irreversibility during cyclic tensile loading, all of which would generate compressive closure loads across the crack faces and shear loads at the crack tips [7, 10]. It is perhaps true to say that the exact way in which the closure loads act to produce mechanical fatigue damage is far from being well understood but there is evidence to suggest that compressive loads, either residual or directly applied across crack faces, tend to produce enhanced fatigue-crack growth rates [17, 21, 28].

There seems now to be little doubt about the susceptibility of brittle materials to cyclic fatigue damage and efforts to understand and categorize fatigue behaviour and fatigue mechanisms in ceramics are well justified. In this paper we present a summary of results obtained in an investigation of the cyclic fatigue properties of some alumina- and zirconia-based ceramics using original techniques especially developed for this purpose.

2. Materials and specimens

The following four ceramic materials produced by Morgan Matroc Limited East Molesey, Surrey, UK, were used in this investigation.

1. Course-grained alumina, commercially known as Deranox 995 which has a purity of 99.5% by mass, a density $> 97\%$ of the theoretical, and an average grain size of 18 μm.

2. High-purity alumina ($> 99.9\%$), known by the commercial name of Vitox, with density of $> 97\%$ of the theoretical. The average grain size is 2 μm, and no traces of any second phase at grain boundaries was detected using high-resolution transmission electron microscopy.

3. Zirconia-toughened alumina (ZTA) based on the Deranox alumina with 20 vol % of dispersed ZrO_2 particles stabilized with 3 mol % fraction of Y_2O_3.

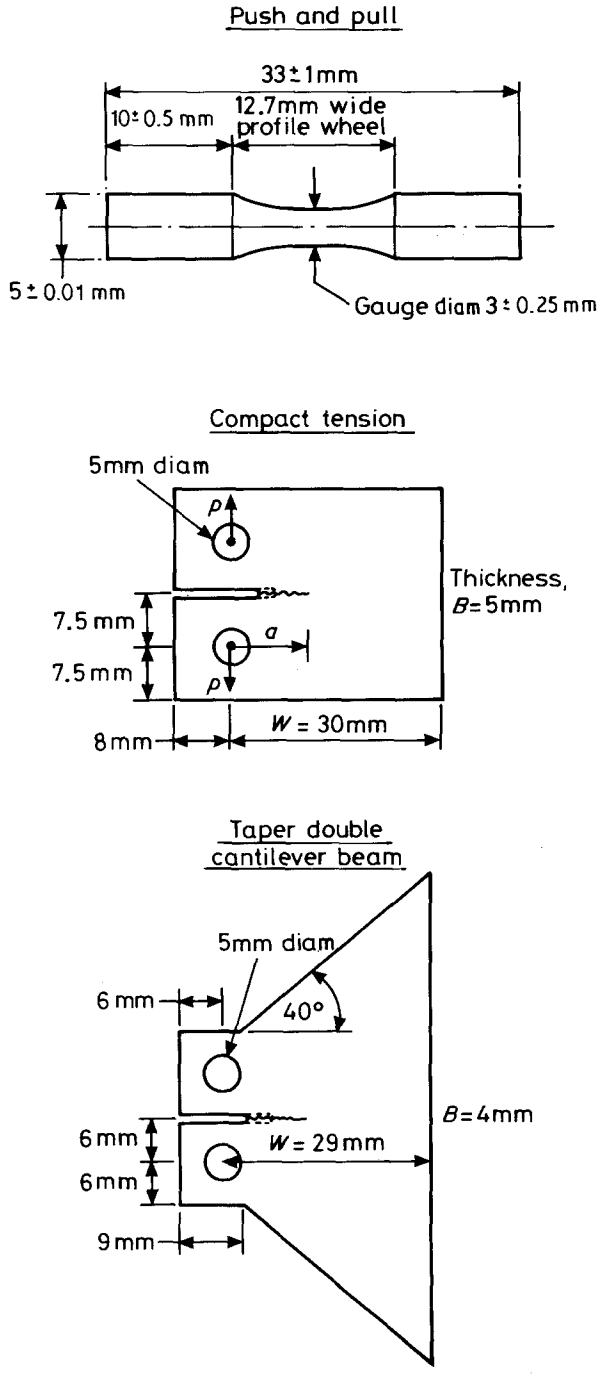

Figure 1 Specimens used in the experiments.

The average alumina grain size is 3.5 μm and the density of the ceramic is > 96% of the theoretical density. X-ray diffraction (XRD) of the surface of the as-fired material revealed the presence of ≈ 7% by volume of monoclinic zirconia phase.

4. Fully stabilized tetragonal zirconia (TZP) containing 3 mol % of Y_2O_3. This has an average grain size of 0.7 μm with occasionally some larger cubic grains of up to 50 μm, and a density of about 99% of the theoretical.

The following specimen geometries were used: push–pull specimens of the shape and dimensions shown in Fig. 1 were accurately machined to strict tolerances using a profiled diamond-impregnated epoxy-bonded wheel of grit size 240. A batch of Vitox specimens was machined with an electroplated diamond wheel of the same grit size. Compact tension, and tapered double cantilever specimens of Deranox alumina were machined in the green state and then finished by surface grinding after firing to the dimensions shown in Fig. 1. Discs for repeated indentation experiments were produced from blanks which were surface ground, lapped and polished to final dimensions of roughly 25 mm in diameter and a thickness of 5 mm.

3. Results

3.1. Push–pull fatigue tests

The push–pull tests were carried out using an improvement of a technique developed and used in the past by one of the authors to fatigue Lucalox alumina [6]. Gripping of the specimens was achieved by friction using split-spring collets in a Mayes servohydraulic machine where the load train had been accurately aligned. With this system, both constant load tests (static fatigue tests) and push–pull fully reversed sinusoidal cyclic stressing, with a stress ratio of $R = -1$ at 5 Hz, were carried out. The results of these tests for the four materials studied are shown in Figs 2 to 5 where the logarithm of the constant stress in the static tests, or the peak stress (σ_{max}) in the cyclic tests, is plotted against the logarithm of both time, t and number of cycles to failure. The experimental data is thus fitted to a relationship of the type

$$\log \sigma_{max} = \frac{1}{n} \log t + C \quad (1)$$

where C and n are constants, and is inconsistent with the relationship

$$v = AK_{max}^{n} \quad (2)$$

with A constant, between the subcritical crack growth rate, v, and the maximum stress intensity factor, K_{max}, [29].

A dependence of this type is commonly accepted to describe the environmentally assisted crack-growth rate under static loads in ceramic materials within a certain velocity range [29], and it has also been used to represent cyclic fatigue-crack growth data [17, 21].

If crack growth were due to environmental effects only, then the time-averaged stress would control the crack-growth rate and the time to failure under static load would be shorter than under cyclic loading.

The ratio between time to failure, t_s, under a static stress, σ_s, and the time to failure t_c, under a fully reversed periodic stress of amplitude, σ_c, is given by [8]

$$\frac{t_c}{t_s} = g^{-1}\left[\frac{\sigma_s}{\sigma_c}\right]^{n} \quad (3)$$

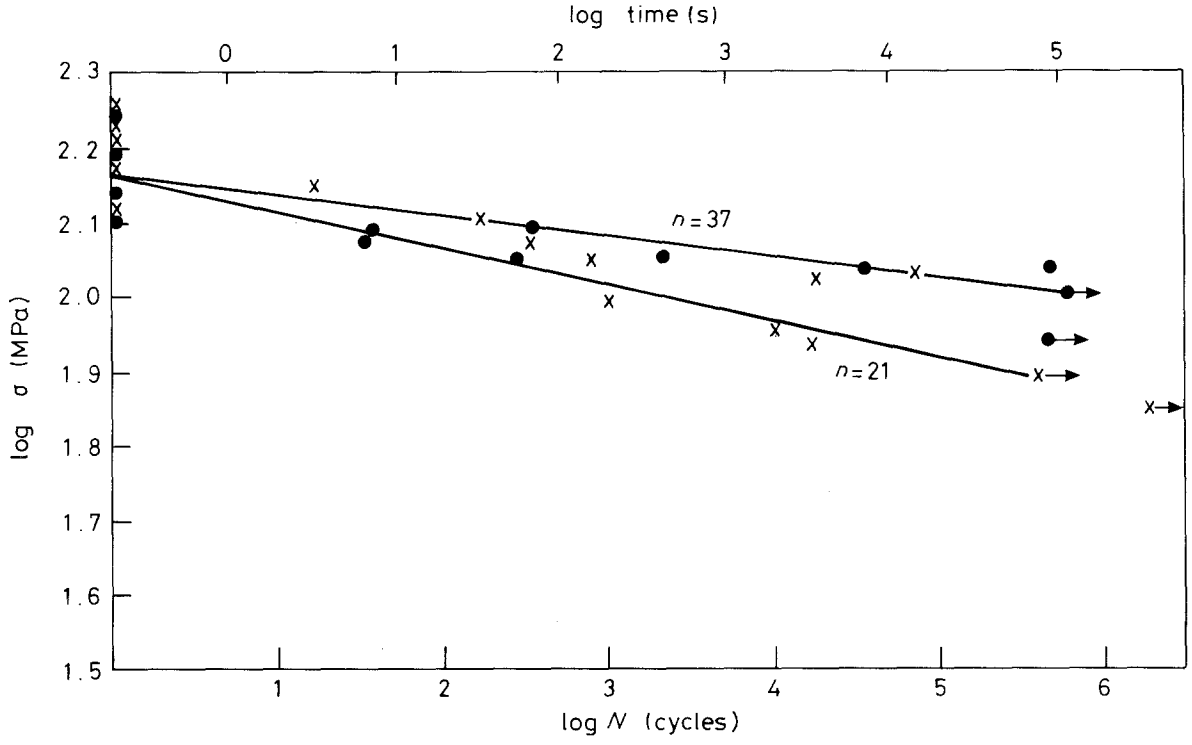

Figure 2 Double logarithmic plot of static stress, or maximum stress against time to failure and number of cycles to failure, for Deranox alumina. •, Static loading; x, cyclic loading with $R = -1$ at 5 Hz.

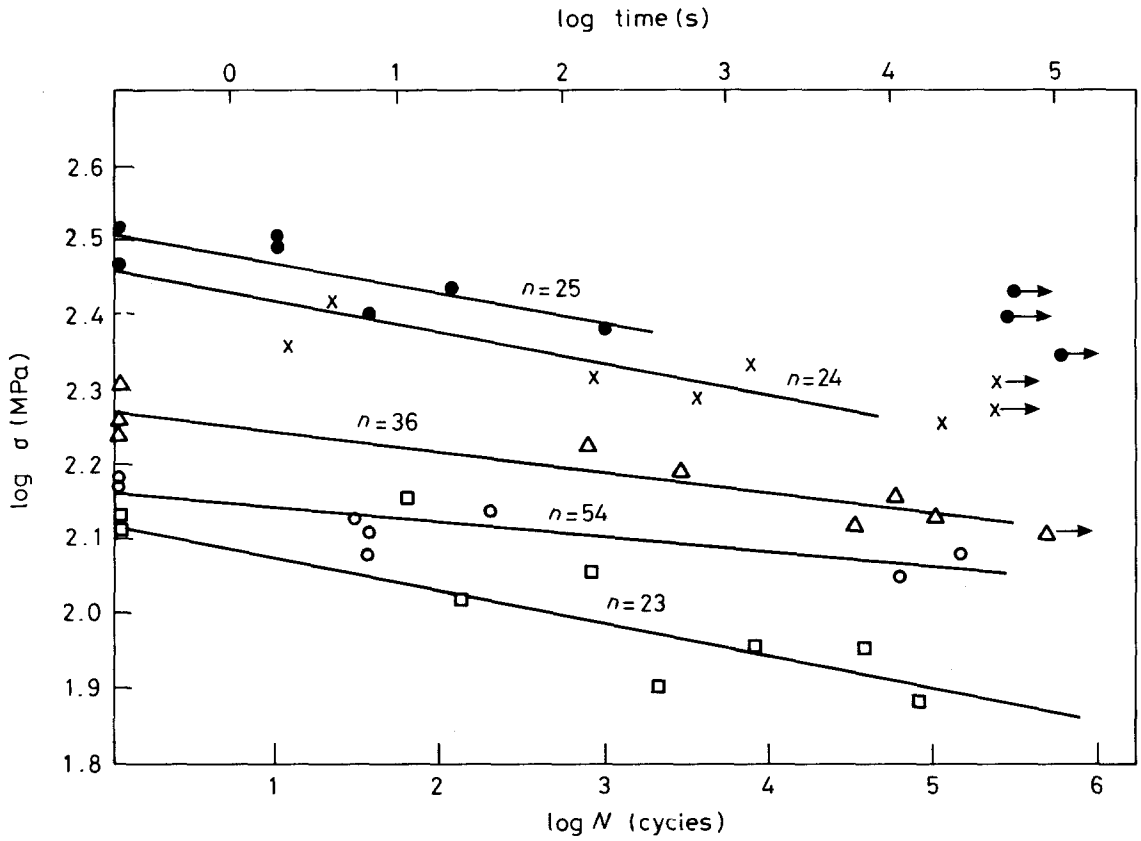

Figure 3 As Fig. 2, for Vitox alumina. △, Static loading, batch 1 (ground); ●, static loading, batch 2 (polished); x, cyclic loading, batch 2 (polished); ○, static loading, batch 3 (ground); □, cyclic loading, batch 3 (ground).

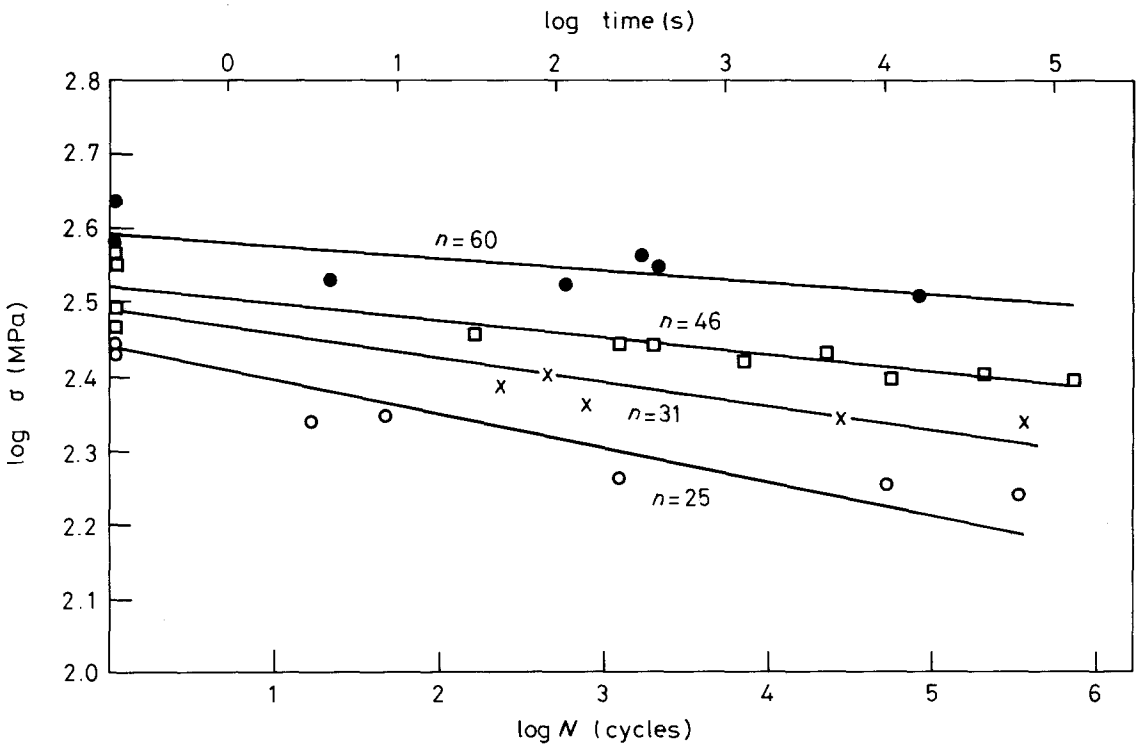

Figure 4 As Fig. 2, for ZTA. □, Static loading, batch 1 (ground); x, cyclic loading, batch 1 (ground); ●, static loading, batch 2 (ground and annealed); ○, cyclic loading, batch 2 (ground).

and for a sinusoidal stress with $R = -1$ as used in our tests [8]

$$g^{-1} = (2\pi n)^{1/2}\left[1 + \frac{1}{4n} + \frac{1}{32n^2} + \ldots\right] \quad (4)$$

Using the smallest value of $n = 30$ for the present results and with $\sigma_s = \sigma_c$, it follows that the times, t_s, to failure under static loads should be at least 13 times shorter than under sinusoidal cyclic loads of the same amplitude. The results show, however, that the cyclic

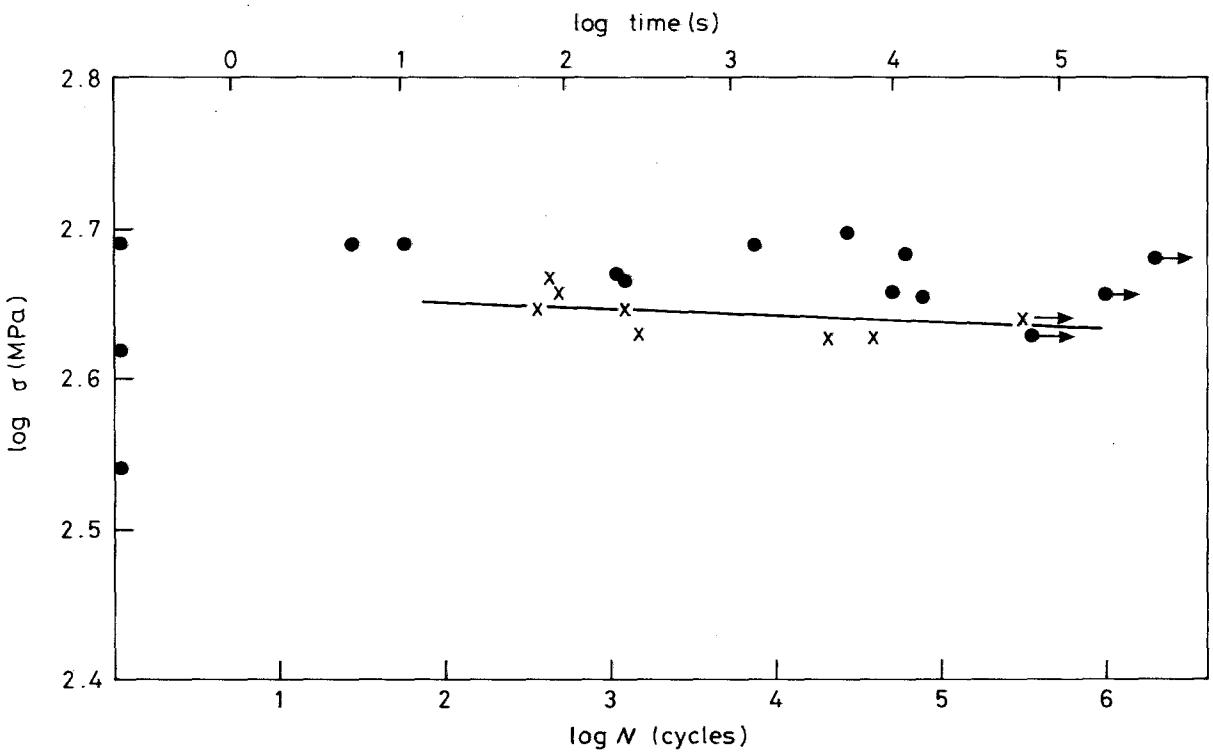

Figure 5 As Fig. 2, for TZP. •, Static loading (ground); x, cyclic loading (ground).

loading produces failure after much shorter times than the static loads, and that the ratio t_s/t_c is not constant but increases with the applied peak stress, revealing the existence of real mechanical cyclic fatigue effects.

The results of the Deranox alumina were obtained with specimens fatigued in the as-machined condition, so that the surface contained grinding scratches which may have provided the fracture origins. However, these fracture origins could not be identified by microscopical examination of the fracture surfaces which were predominantly intergranular. No differences between regions of slow crack growth and fast fracture were distinguishable. The static and cyclic values of n obtained from the plots of Fig. 2 are comparable to those obtained for the same and similar materials, using a different technique [21].

The results for the Vitox alumina were obtained with three different specimen batches, as indicated in Fig. 3. Batches 1 and 2 refer to as-ground specimens which were machined using different types of grinding wheels (see section 2). The specimens of batch 2 were polished after grinding, using successively finer diamond grades and finished with a 1 μm paste after having removed about 250 μm from the ground surface.

The results presented in Fig. 3 show that the fatigue behaviour is very sensitive to the condition of the specimen surface. This dependence is probably due to the severity and type of surface flaws existing in the unpolished specimens, as well as the possible residual machining surface stresses. A dramatic increase in strength is achieved by polishing the machined surface layer, as a result of having reduced the largest flaw size.

All the fracture surfaces of the Vitox samples exhibited fracture mirror features, and the failure origins could all be traced to surface flaws. These flaws in the unpolished samples were surface cracks similar to the median-radial cracks formed beneath sharp indenters [30]. A transition between a mainly intergranular region of slow crack growth and a transgranular fast fracture surface could be identified, as in Fig. 6. It was clearly evident from these observations that in the polished samples the size of the surface flaws had been greatly reduced.

A pronounced batch variability was also evident in the results of the ZTA specimens (Fig. 4). The two batches of the as-ground specimens were machined with the same grinding wheel but at different times and by a different operator. A third batch of specimens was annealed, after machining, for 1 h at 1450 °C. This treatment resulted in a dramatic increase in strength. The annealing treatment probably produces two different effects. One is the healing of the micro-cracks resulting from both the ZrO_2 tetragonal–monoclinic phase transformation on grinding and from the mechanical damage itself [31]. The other effect is the reduction in the amount of transformed ZrO_2 particles and the annealing out of the compressive stresses at the specimen surface [32, 33]. X-ray intensity measurements performed on flat specimens of ZTA subjected to the same grinding and annealing operations showed that the volume fraction of transformed monoclinic ZrO_2 increased to 67% after surface grinding followed by slight polishing, and that after annealing it had been reduced to 35%. Although surface grinding has been shown to increase the strength of ZTA [34–36] because of the formation of compressive surface stresses, the present results show that as far as fatigue strength is concerned, removal of surface flaws by annealing may be more beneficial than maintaining the machined compressive layer. A

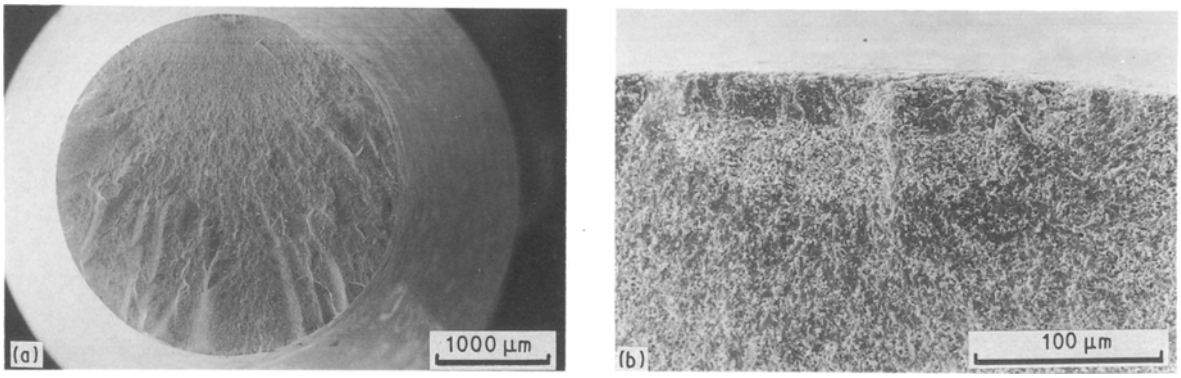

Figure 6 Cyclic fatigue fracture surface of Vitox alumina, (a) showing fracture origin, (b) showing transition between stable and unstable crack regions.

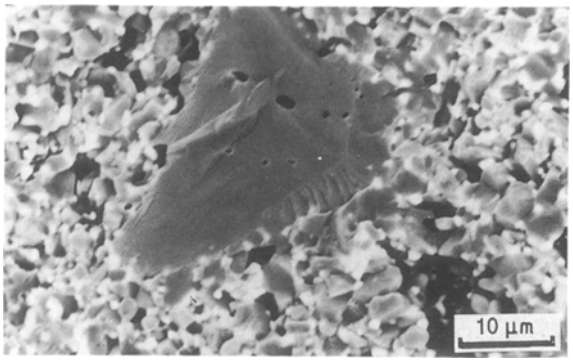

Figure 7 Large alumina grains where fracture is initiated in annealed ZTA specimens.

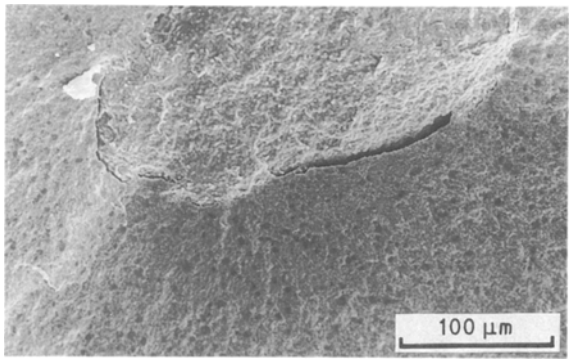

Figure 8 Internal cracks as fracture origins in TZP specimens.

combination of both probably exists which produces maximum improvement of fatigue properties.

Fracture origins could always be identified in batches 1 and 2, and these were always associated with surface cracks produced by machining damage, but regions of slow crack growth were not discernible. The fracture surfaces were mainly intergranular. In the annealed samples fracture was always initiated at interior flaws, and not at the surface. These fracture origins were mainly exceptionally large alumina grains, or large pores produced by poorly sintered regions (Fig. 7).

In the TZP samples, the fracture invariably originated at bulk interior defects. These were mainly flattened pores, or unsintered agglomerates of 50–150 μm in size with transgranular cracks associated with them (Fig. 8). The large value of $n \approx 100$ for the static data and a large scatter in strength values for the cyclic tests is probably due to the nature of the critical flaws, which in this material have a wide size distribution.

3.2. Slow crack-growth experiments

Measurements of slow crack-growth velocities were made in Deranox alumina using the specimen geometries shown in Fig. 1. The cracks were started at the root of a pre-machined notch by forcing a wedge into the notch. The specimens were subsequently fatigued with a fully reversed sinusoidal load, i.e. load ratio $R = P_{min}/P_{max} \approx -1$, at frequencies of 5 and 10 Hz. The value of the maximum load, P_{max}, was chosen to produce an initial slow crack-growth rate which increased during the test as the cracks grew longer and the magnitude of the maximum stress intensity factor K_{max} increased. The crack length was measured on both the specimen surfaces with a travelling microscope. Although the crack lengths usually differed by a few millimetres on each side of the specimen, the cracks grew at the same rate during the tests. At regular intervals during the cyclic fatigue tests a static tensile load equal to P_{max} was applied to the samples for long periods, and it was observed that no static crack growth occurred over a large interval of K_{max} values within which the cracks grew by cyclic fatigue.

Double logarithmic plots of crack growth rate against K_{max} are shown in Fig. 9. In these figures the growth rates under cyclic and static loads can be compared. It is clear that under cyclic fatigue the cracks grow faster and at lower values of K_{max} than under static fatigue, and that the results are independent of loading frequency. It should also be noted that the slopes of the plots in these figures are different for the two specimen geometries used, and that for the same value of P_{max} and K_{max} the cracks grow at faster rates in the tapered specimens than in the compact tension specimens. Some suggestions on a possible interpretation of these results have been advanced elsewhere [21] on the basis of the effects of compressive loads acting on the asperities of the crack faces. The implication of that interpretation is that in these types of point-loaded specimens the crack velocity seems to be an increasing function of crack length.

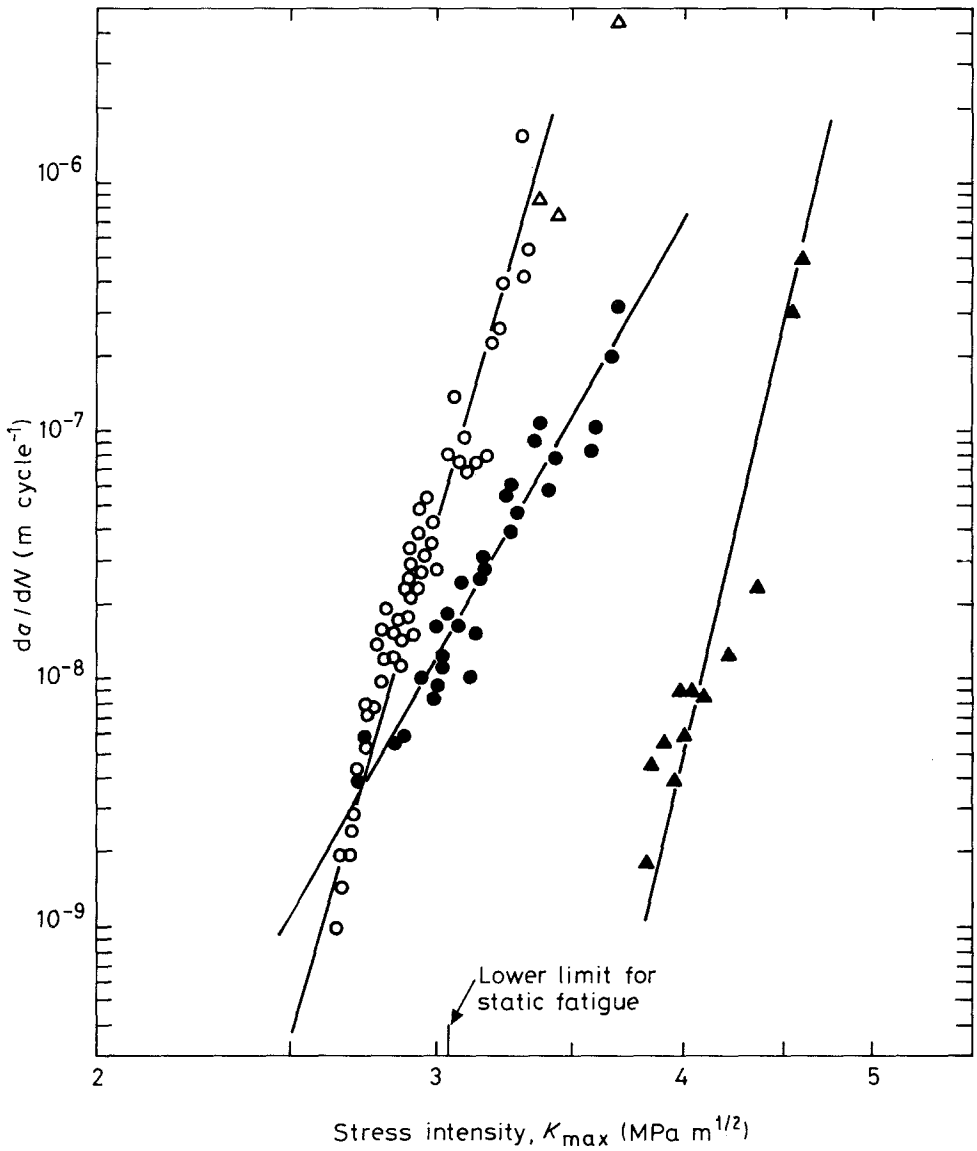

Figure 9 Double logarithmic plots of crack-growth rate against maximum stress-intensity factor for two specimen types. o, cyclic; ▵, static; open symbols, tapered double cantilever beam; closed symbols, compact tension.

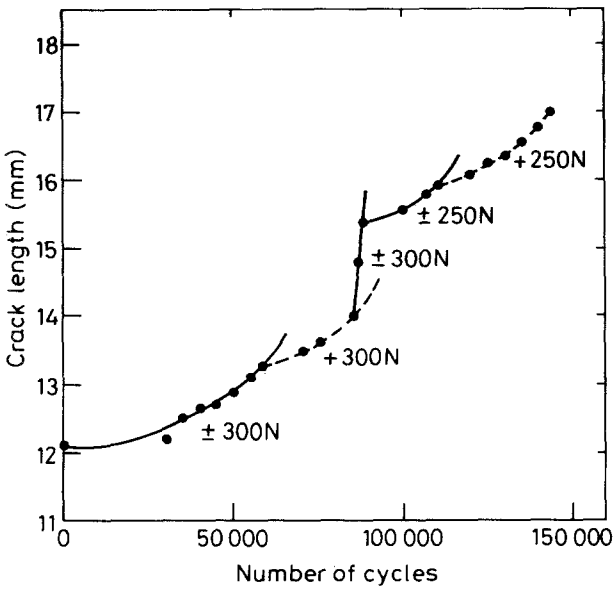

Figure 10 Plot of crack length against number of cycles for a cyclically loaded, tapered cantilever specimen. Note the effect of compressive load on crack-growth rate. (——) $R = -1$; (– – –) $R = 0$.

This dependence is contrary to that expected from a material which exhibits a "crack-resistance curve" (or *R*-curve) behaviour [33, 37–40].

The values of the exponent n obtained with compact tension specimens (Fig. 9) are $n = 14$ for the cyclic fatigue and $n = 33$ for the static fatigue. The value of n for static fatigue agrees with that obtained from the push–pull test for the same Deranox alumina. However, it is significantly different for cyclic fatigue.

To investigate the direct effect of the compressive component of the cyclic load on the crack-growth rate, a test was carried out with a tapered cantilever specimen subjected to cyclic loading where R was varied between -1 and 0 during the test whilst keeping the same maximum tensile load. The results of the test are shown in Fig. 10 where it can be seen that the crack-growth rate increases whenever R is changed from zero to -1, whereas it decreases when R is changed from -1 to zero.

Attempts to precrack specimens and to grow stable cracks by cyclic or static fatigue in other materials were unsuccessful. While there is an inherent difficulty in introducing a stable "through thickness" crack in

thick specimens like those used in our experiments, it is not obvious why this should be easier in the Deranox alumina for which the value of the exponent n is not smaller than for the other materials. Hence the stability of a slowly growing crack seems to depend more on the microstructure of the material than on the actual value of the exponent n.

Specimen geometries giving constant or decreasing values of K_I with increasing crack length [8, 9, 27] should be more suitable to measure stable crack-growth rates. These geometries have the disadvantage of greater difficulty in subjecting the cracks to negative values of load ratio R, i.e., tension–compression loads. This is an unfortunate restriction for fatigue studies since our results have shown that the crack-growth rate depends on the magnitude of R in such a way that for the same values of K_{max}, increasing the compressive component of the load increases the growth rate.

3.3. Repeated indentation tests

A simple technique based on the repeated indentation of a polished surface with a Vickers diamond indenter was developed to study cyclic fatigue in ceramics. A detailed analysis of the technique is reported elsewhere [28]. The method consists of producing a standard indentation cavity with a standard load or pre-load, P, and this cavity is then repeatedly indented with a load $P' \leq P$ until chipping (or spalling) of the material around the indentation occurs. The pre-load, P, produces a system of radial and lateral cracks which are subjected to residual tensile forces. The residual force on the lateral cracks acts outwards normal to the surface at the centre of the indentation cavity (Fig. 11) and it has a maximum value, P_{ro}, when the crack is fully closed, and a minimum value, P_r, when the crack is relaxed and open. When the indentation cavity is repeatedly loaded with a force, P', the force on the lateral cracks varies from P_r to $P_{ro} - P'$. While P_r is always tensile, $P_{ro} - P'$ can be compressive if $P' > P_{ro}$. Thus in the repeated indentation tests the lateral cracks can be subjected to reversed cyclic loads which drive them by fatigue to the surface to produce chipping or spalling.

The most complete set of results on repeated indentation were obtained with polished disks of Vitox alumina [28]. The incidence of chipping was detected with an acoustic emission technique using a Dunegan/Endevco 4103 activity monitoring system. An average signal level output was displayed on a recorder. An acoustic emission peak was detected on the first indenter loading and another peak on unloading, the latter probably corresponding to the formation of the lateral cracks. After a number of indentation cycles a peak was observed which corresponds to the incidence of chipping (Fig. 12).

The results of the tests on Vitox alumina are shown in Fig. 13, where the number of indentation cycles needed to produce chipping are plotted against the repeated indentation load, P', for several values of pre-indentation load, P. The number of cycles to chipping is a function of P', and there is a threshold value of P' below which no chipping occurs. This is like a fatigue limit which increases with the magnitude of the standard pre-indentation load P.

The radial cracks, associated with the pre-indentation, were never seen to grow during the repeated indentation tests and no chipping could be produced by letting the indenter dwell under load on the indentation cavity for periods of time in excess of 24 h. This confirms that the lateral cracks were driven to the surface by cyclic fatigue effects.

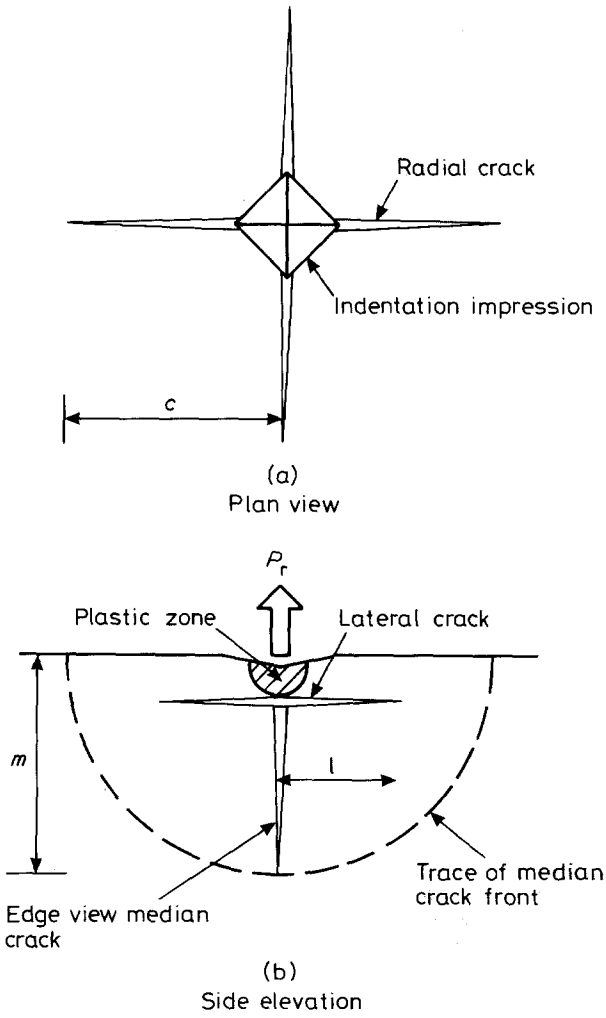

Figure 11 Schematic representation of crack systems produced by a sharp indenter.

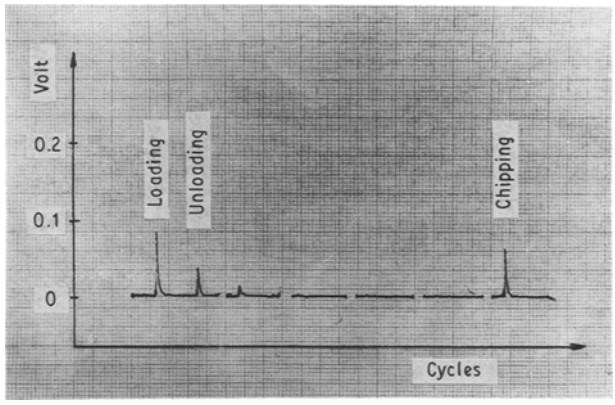

Figure 12 Record of acoustic emission signals produced on repeatedly indenting a surface of Vitox alumina

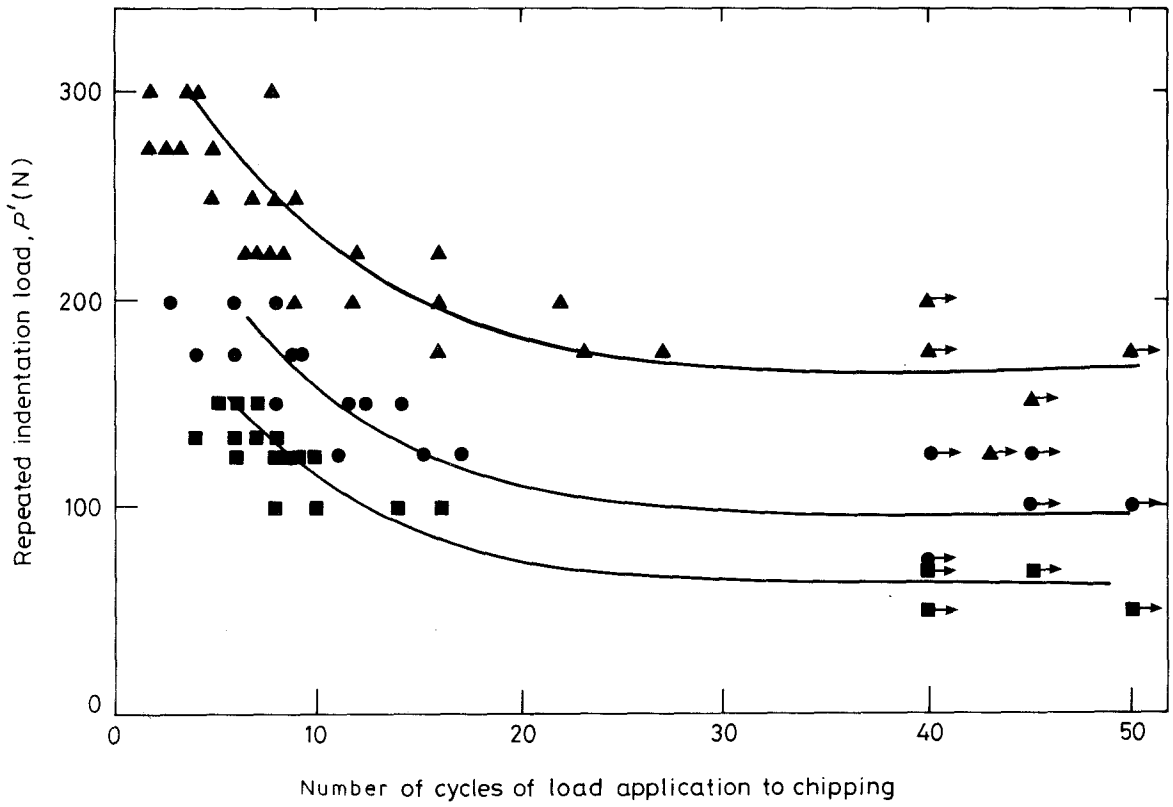

Figure 13 Results of repeated indentation tests obtained with Vitox alumina. P = ▲, 300; ●, 200; ■, 150 N.

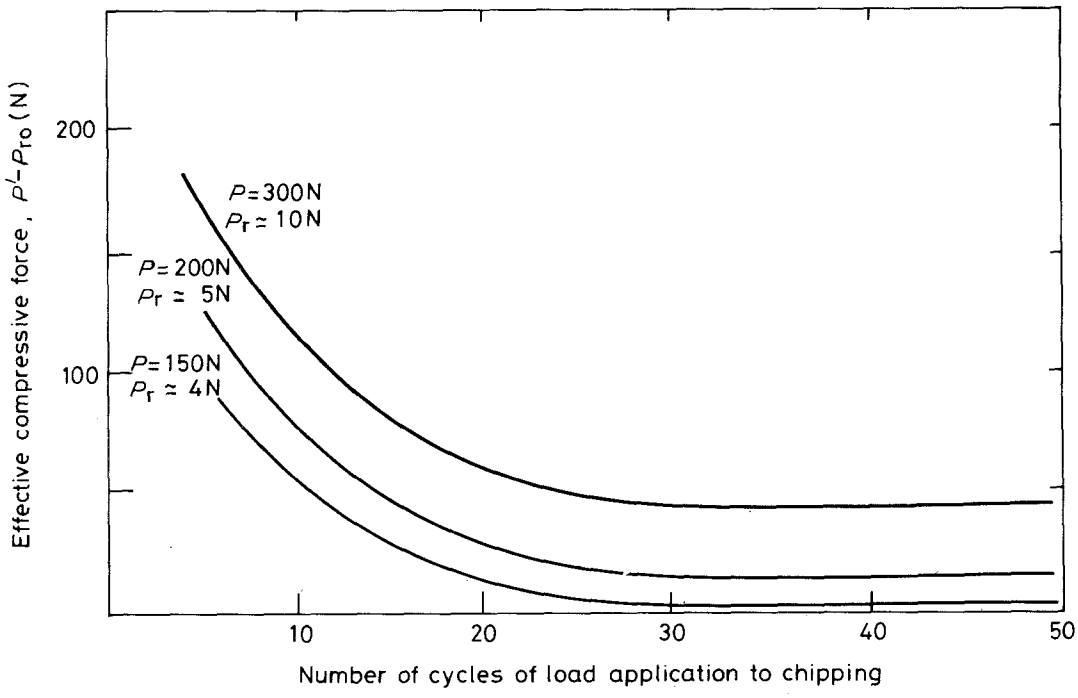

Figure 14 Same results as in Fig. 13, plotted in terms of the effective compressive component across the lateral crack faces. Values of residual tensile component indicated in figures.

An analysis of the technique using elastic/plastic theory has made it possible to estimate that for high-strength ceramic material $P_{ro} \approx 0.4P$, and that the residual tensile load P_r is of the order of 3% of the pre-indentation load P [28]. By repeated indentation with a load P' the lateral cracks are subjected to cyclic forces whose maximum value is $0.03P$ and the minimum value is, $0.4P - P'$. The cracks are therefore cyclically fatigued with a load ratio $R = (0.4P - P')/0.03P$. By re-plotting the results of Fig. 13 in terms of the effective load, $0.4P - P'$ across the lateral crack faces, the curves of Fig. 14 are obtained. It can be seen that the threshold levels, or fatigue limits, of Fig. 14 correspond to negative values of R implying that compressive forces across the crack faces are needed to produce chipping. This seems to confirm a

recurring pattern in cyclic fatigue in ceramics, namely that crack closure or compressive loads across the crack faces are needed to produce subcritical crack growth by cyclic fatigue.

Repeated indentation tests could not be carried out on a ground and polished surface of ZTA. A large single acoustic emission peak was detected on the first indentation and this corresponded to massive chipping of the surface around the indentation cavity [11, 41]. This behaviour was even observed to occur for indentation loads as small as 50 N. When an as-fired surface of ZTA disk was not ground, but only slightly and carefully polished to produce a good enough finish for surface indentation, clean indentations could be produced, and repeated indentation tests were carried out on these surfaces. These indentations produced acoustic emission signals during both the loading and unloading parts of the indentation cycle, similar to those obtained in the indentation of Vitox alumina. The results of repeated indentation tests on a lightly polished and untransformed surface of ZTA with pre-indentation loads of 100, 200 and 300 N are shown in Fig. 15, where the number of cycles to chipping are plotted against the effective compressive force, as for Vitox alumina in Fig. 14. The curves for ZTA are flatter than those corresponding to Vitox alumina and the threshold levels of compressive load for chipping are significantly higher. This seems to reflect a greater fatigue resistance for the ZTA material in agreement with the results obtained from the push–pull tests.

It should be noted that our calculation of the effective compressive force is based on the assumption that the residual forces and surface uplift at the indentation are produced by the hemispherical plastic zone beneath the indentation. This is obviously not satisfied in easily transformable zirconia ceramics where relatively large uplifts occur at the indentation as a result of the transformation. Since the volume fraction of transformable zirconia is small in our ZTA material, and no anomalous uplift was observed in the indentation tests, the curves of Fig. 15 have been obtained neglecting any transformation effects.

The tetragonal–monoclinic transformation of the ZrO_2 particles induced by grinding, and the resultant compressive stresses generated at the surface, have been found to increase the flexural strength of ZTA [34–36]. The present results show, however, that surface grinding may not always be beneficial to the mechanical properties of ZTA. In particular, the presence of compressive surface stresses, and possibly micro-cracks that may have been induced by the phase transformation, are detrimental to the strength of the surface when it is subjected to complex contact and point-loading conditions, as in indentation. This could also have important implications for surface related mechanical properties such as abrasion and wear.

Single indentation of a ground and polished surface of Deranox alumina always resulted in chipping of the indentation cavity. This behaviour was not investigated further, so it is not known whether this is due to intrinsic quality of the material or to the presence of residual stresses, or remnant surface flaws, produced by grinding.

The indentation of a ground and polished surface of TZP with loads of up to 500 N always produced sharp indentations with a well developed system of radial

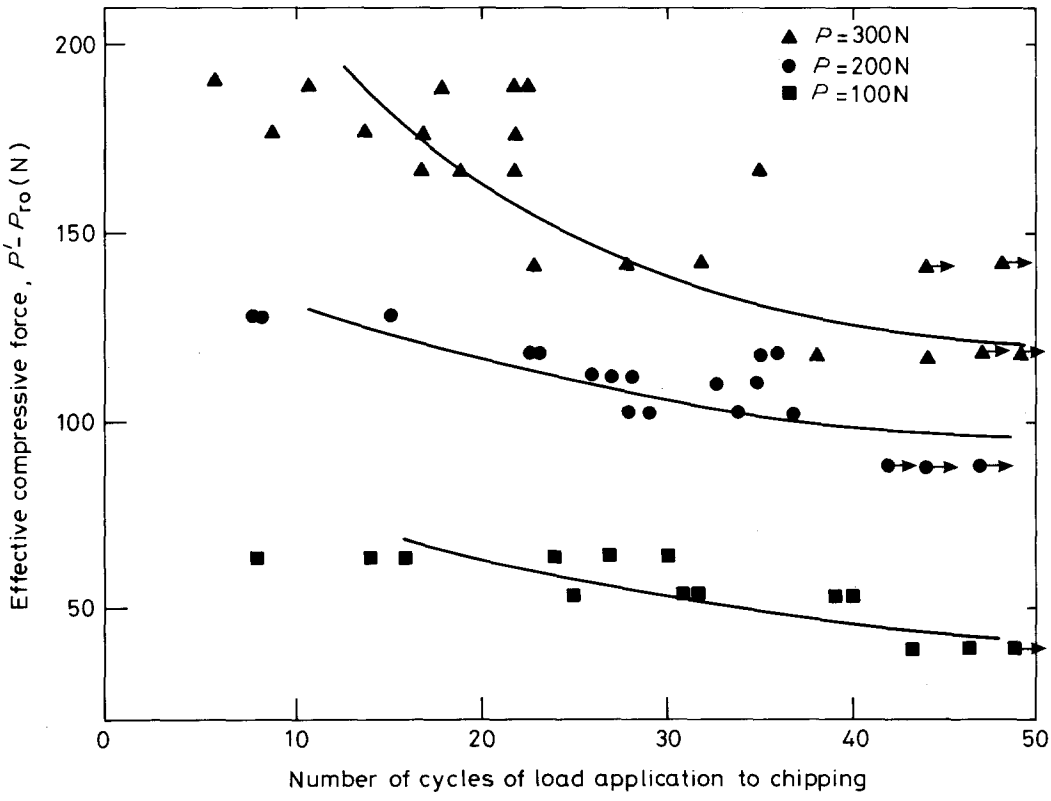

Figure 15 Results of repeated indentation tests carried out on a polished sample of ZTA. Data plotted in terms of effective compressive force across the lateral crack faces.

cracks. Only one acoustic emission peak was detected on loading, and none on unloading. Repeated indentation for as many as 120 cycles with 500-N loads did not produce any spalling at the indentation cavity. This does not mean that this material was not susceptible to cyclic fatigue, but rather suggests (together with the acoustic emission observations) that a system of lateral cracks was not produced by the indentation loads used because of the relatively high toughness of TZP (which has a value of 6 MPa $m^{1/2}$ when measured from the length of indentation radial cracks). Observations on indentation profiles made subsequently by one of the authors (M. J. R., unpublished results) confirmed that no lateral cracks are formed in this material with indentation loads as high as 300 N.

4. Discussion

Three methods have been used in the present investigation to examine different aspects of the cyclic fatigue behaviour of ceramics. They provide complementary information on the stable growth of subcritical cracks under cyclic loading conditions, and all the results obtained confirm the existence of mechanical cyclic fatigue effects in the materials used.

Although it seems to be possible to establish some correlation between the fatigue results obtained with the three different testing methods used in the present investigation, this has to be done with some care. In the push–pull tests the fatigue failure of the samples is dictated by the behaviour of short and mainly surface cracks that grow over a short distance before they attain the critical size for failure under the test conditions. The conditions involved in the growth of these cracks may be different from those relevant to the slow stable growth of the long and large front cracks examined in the compact tension and double cantilever tests. For instance, it is necessary to consider the effect of crack length on the apparent value of fracture toughness which gives rise to the so called *R*-curve behaviour, particularly in materials that have a coarse microstructure [37–40].

The repeated indentation tests, on the other hand, provide information about the growth of sub-surface cracks with a particular configuration, i.e. lying parallel to the specimen surface. Their behaviour under cyclic loading may be influenced by factors which are not present in cracks which propagate in a direction normal to the far-field loads and into the bulk of material. Even when all these considerations are taken into account, one common aspect emerging from all the results available for the cyclic fatigue of ceramics is that compressive forces, residual or direct, across the crack faces seem to be always associated with the cyclic fatigue, producing enhanced crack-growth rates and hence shorter failure-times.

This observation suggests a possible explanation for the cyclic fatigue effects in ceramics, based on existing interpretations of the stable growth of cracks under static loads and the *R*-curve behaviour of some ceramic materials. Both these effects have been adequately explained for coarse-grained materials in terms of the bridging of the crack faces by unbroken grains, or grains restrained by frictional forces, in the wake of the advancing crack tip [38, 40]. Because this is essentially a microstructural effect it will be independent of the mode of loading: in other words, the growth rate of a stable crack, whether under static or cyclic loading, will depend on the number of bridging ligaments behind the crack front, the strength of the ligaments and their distribution behind the crack tip. The crack will advance as bridging ligaments are broken behind the crack tip, and it is tempting to suggest that the effect of cyclic loading is that of degrading or helping to break bridging ligaments, either by repeated fretting, shear or crushing, arising from stress reversal and residual or direct compressive loads on the crack faces. This would provide a reasonable explanation for the cyclic fatigue growth of long cracks in materials where stable crack growth is easily achievable, as in our experiments with Deranox alumina which has a coarse microstructure. It would also imply that the effects of cyclic fatigue on crack growth should be more noticeable in materials exhibiting pronounced *R*-curve behaviour arising from crack bridging.

This interpretation is not inconsistent with the results of the push–pull tests where failure occurs by the catastrophic propagation of the small surface cracks after a very short regime of subcritical crack growth. Crack bridging by unbroken ligaments behind the crack tip develops as the crack grows and it produces a negative stress intensity factor, K_b, which subtracts from that due to the external load, K_a, thus reducing the actual or effective value of the local stress intensity, K_I, at the crack tip. Stable subcritical crack growth can proceed for as long as K_I remains smaller than a critical value K_{IC} characteristic of the material. The rate at which K_a increases with the crack length (normalized with respect to specimen dimensions) under constant load depends strongly on the geometry of the sample, and it is much faster for a surface crack in a push–pull specimen than for a crack at the tip of a notch in a compact tension specimen. Hence in a push–pull specimen of small size the instability will be reached when the crack is still short and before it has had a chance to develop any bridging.

Other mechanisms have been suggested to account for the effect of cyclic loading on crack growth. These are mainly crack-tip processes based on the arrest and re-activation of the crack front by repeated kinking [10], or by the release of internal stresses [7], upon load reversal. There is, as yet, no conclusive evidence to support any of these alternative interpretations. It is even possible that different mechanisms, or a combination of different mechanisms, can be operative in different materials. However, if cyclic fatigue effects are exclusively due to local crack-tip mechanisms, then it is to be expected that the measurable cyclic fatigue parameters, like crack-growth rate and exponent *n*, would depend only on the value of the stress intensity factor, K_a, produced by the external load. If, on the other hand, crack bridging or other crack wake effects such as wedging or levering by asperities are important, then the cyclic fatigue behaviour as well as crack resistance and apparent fracture toughness will be

dependent on both specimen geometry, specimen size and crack length.

5. Conclusions

1. Three different methods have been used to investigate the cyclic fatigue behaviour of ceramics. The results obtained with the three methods show that coarse-grained alumina, fine-grained alumina of high purity, ZTA and TZP are all susceptible to mechanical cyclic fatigue effects.

2. The times to failure in direct push–pull under cyclic loads are considerably shorter than times to failure under static loads of the same magnitude for all the materials studied. The very sensitive effect of surface condition on both static and cyclic strength has been demonstrated.

3. Crack growth rates in coarse-grained alumina under cyclic loads are significantly faster than under static loads. The relation between crack-growth rate and maximum value of the stress intensity factor has been found to depend on specimen geometry.

4. The results of cyclic fatigue by repeated indentation can be correlated with those obtained in push–pull for fine-grained alumina and zirconia-toughened alumina.

5. In all the tests there is evidence to suggest that cyclic compressive loads across the work faces produce enhanced crack-growth rates. An explanation is suggested for the growth of cracks in cyclic loading in terms of the effect of compressive loads on the degradation of ligaments bridging the crack faces.

Acknowledgements

The authors are grateful to the Science and Engineering Research Council (SERC) and Harwell Laboratory of the UK Atomic Energy Authority for financial support of a research programme on the cyclic fatigue of ceramics.

References

1. L. S. WILLIAMS, *Trans. Brit. Ceram. Soc.* **55** (1956) 287.
2. *Idem*, in "Mechanical Properties of Engineering Ceramics", edited by W. W. Kriegel and H. Palmour III (Interscience, New York, 1961) p. 245.
3. B. K. SARKAR and T. G. T. GLINN, *Trans. Brit. Ceram. Soc.* **69** (1970) 199.
4. D. A. KROHN and D. P. H. HASSELMAN, *J. Amer. Ceram. Soc.* **55** (1972) 208.
5. C. P. CHEN and W. J. KNAPP, in "Fracture Mechanics of Ceramics", edited by R. C. BerBradt, D. P. H. Hasselman and F. F. Lange (Plenum, New York, 1974) p. 691.
6. F. GUIU, *J. Mater Sci.* **13** (1978) 1357.
7. D. LEWIS and R. W. RICE, *Ceram. Engng Sci. Proc.* **3** (1982) 14.
8. A. G. EVANS and E. R. FULLER, *Met. Trans.* **5** (1974) 27.
9. A. G. EVANS and M. I. LINZER, *Int. J. Franct. Mech.* **12** (1976) 217.
10. A. G. EVANS, *Int. J. Fract. Mech.* **16** (1980) 485.
11. F. GUIU and D. A. J. VAUGHAN, in "Processing of Advanced Ceramics", edited by J. S. Moya and S. de Aza (Sociedad Española de Cerámica Vidrio, Madrid, 1986) p. 217.
12. K. KIM and A. MUBEEN, American Society for Testing and Materials, Special Technical Publication 745 (1981) p. 157.
13. T. KAWAKUBO and K. KOMEYA, *J. Amer. Ceram. Soc.* **70** (1987) 400.
14. H. N. KO, *J. Mater. Sci.* **6** (1987) 175.
15. V. ZELIZKO and M. V. SWAIN, *ibid.* **23** (1988) 1077.
16. H. N. KO, *ibid.* **5** (1986) 464.
17. R. H. DAUSKARDT, W. YU and R. O. RITCHIE, *J. Amer. Ceram. Soc.* **70** (1987) 248.
18. L. A. SYLVA and S. SURESH, *J. Mater. Sci.* **24** (1989) 1729.
19. R. H. DAUSKARDT, D. B. MARSHALL and R. O. RITCHIE, *J. Amer. Ceram. Soc.* **73** (1990) 893.
20. L. X. HAN and S. SURESH, *ibid.* **72** (1989) 1233.
21. M. J. REECE, F. GUIU and M. F. R. SAMMUR, *ibid.* **72** (1989) 348.
22. P. AGATONOVIC and R. GRUNMACH, *Vortrage Werkstoffprufung, D.V.M.* (1987) 95.
23. L. E. EWART and S. SURESH, *J. Mater. Sci. Lett.* **5** (1986) 774.
24. L. E. EWART and S. SURESH, *J. Mater. Sci.* **22** (1987) 1173.
25. S. SURESH, L. X. HAN and J. J. PETROVIC, *J. Amer. Ceram. Soc.* **71** (1988) C158.
26. S. SURESH and J. R. BROKENBROUGH, *Acta. metall.* **36** (1988) 1455.
27. A. GROSSMÜLLER, V. ZELIZKO and M. V. SWAIN, *J. Mater. Sc. Lett.* **8** (1989) 29.
28. M. J. REECE and F. GUIU, *J. Amer. Ceram. Soc.* **73** (1990) 1004.
29. A. G. EVANS and S. M. WIEDERHORN, *Int. J. Fract. Mech.* **10** (1974) 379.
30. B. R. LAWN, A. G. EVANS and D. B. MARSHALL, *J. Amer. Ceram. Soc.* **63** (1980) 574.
31. D. J. GREEN, *ibid.* **65** (1982) 610.
32. S. HORI, M. YOSHIMURA and S. SOMIYA, *ibid.* **69** (1986) 169.
33. A. H. HEUER, *ibid.* **70** (1987) 689.
34. D. J. GREEN, F. LANGE and M. R. JAMES, in "Advances in Ceramics Science and Technology, Zirconia II", edited by A. H. Heuer and L. W. Hobs (American Ceramic Society, 1984) p. 240.
35. R. T. PASCOE, in "Ceramic Microstructures", edited by R. M. Fulrath and J. A. Pask (Westview Press, 1977) p. 774.
36. T. K. GUPTA, *J. Amer. Ceram. Soc.* **63** (1980) 117.
37. P. L. SWANSON, C. J. FAIRBANKS, B. R. LAWN, Y-W. MAI and B. J. HOCKEY, *ibid.* **70** (1987) 289.
38. Y-W. MAI and B. R. LAWN, *ibid.* **70** (1987) 279.
38. Y-W. MAI and B. R. LAWN, *ibid.* **70** (1987) 279.
39. R. W. STEINBRECH and O. SCHMENKEL, *ibid.* **71** (1988) C-271.
40. S. J. BENNISON and B. R. LAWN, *Acta Metall.* **37** (1989) 2659.
41. D. A. J. VAUGHAN and F. GUIU, *Brit. Ceram. Proc.* **39** (1987) 101.

Received 8 June
and accepted 29 October 1990